

Global phase diagrams for dipolar fluids

H. Zhang and M. Widom

Department of Physics, Carnegie Mellon University, Pittsburgh, Pennsylvania 15213

(Received 7 March 1994)

Fluids of molecules or particles interacting through dipole forces describe polar liquids and colloidal suspensions such as ferrofluids and electrorheological fluids. Phase diagrams for systems with strong dipolar coupling are not precisely known. Possible liquid state phase transitions include phase separation and spontaneous polarization. We present a set of generic phase diagrams for the fluid states of dipolar spheres and spheroids, focusing on the interplay of polarization and phase separation.

PACS number(s): 61.25.Em, 64.60.Cn, 75.50.Mm, 64.70.Fx

Dipolar forces influence a wide spectrum of fluids, from fluids of polar molecules [1], where the dipolar interaction is electrostatic, to ferrofluids [2], where it is magnetostatic. The strength of dipolar coupling also differs widely in different fluids. In many dipolar fluids, three dominant interactions determine the thermodynamics: short-ranged repulsion, long-ranged dipole-dipole interaction, and the dispersive van der Waals attraction [3]. When the dipolar coupling is weak, it is treated only as a perturbation to the dispersive attraction [4-7], in the form of its orientational average, with a van der Waals-like $1/r^6$ attraction as its leading term. But strongly coupled dipolar fluids such as ferrofluids exhibit unusual phenomena from particle chaining [4,9-11] to field induced phase separation [12,13]. Most exciting is the possibility of fluids with ferromagnetic order [14-16], which have never been observed experimentally.

Phase diagrams for dipolar fluids remain only partially understood. The widely studied dipolar hard sphere model may display phase separation as suggested by its solution via the mean spherical approximation [5,17]. More likely it displays a magnetized liquid state as suggested by recent computer simulations [10,18]. No theory to date has examined the interplay of these two possibilities. The story is similar for dipolar soft spheres [13,19] and for variants of the Stockmayer fluid [11,20] which add $1/r^6$ attraction to the soft sphere $1/r^{12}$ repulsion.

Real polar molecules (e.g., H_2O) and ferrofluids with strong dipolar couplings [3] do exhibit phase separation into dilute gas and dense liquid phases at appropriate temperatures and densities. Never has spontaneous polarization been confirmed in the liquid state.

In this paper we introduce generic phase diagrams for dipolar fluids that connect spontaneous polarization with isotropic phase separation. Since we focus on fluid states, we ignore any competition from solid phases which might preempt some of the transitions described below. And we consider spherical (or nearly spherical) particles, so we ignore nematic liquid crystalline states. Our free energy contains four terms:

$$\frac{F[\rho, m]}{Nk_B T} = \ln \frac{\rho}{1 - \rho/3\rho_c^0} - \frac{9\rho/\rho_c^0}{8T/T_c^0} + e(m) - \frac{2\pi}{3T} \rho m^2, \quad (1)$$

where m is the magnetization per particle ($0 \leq m \leq 1$),

ρ is the particle density. All scales are set in relation to particle dipole moment $\mu = 1$ and particle diameter $a = 1$. The first two terms represent a van der Waals fluid with critical point for phase separation into an isotropic gas and an isotropic liquid placed at ρ_c^0 and T_c^0 . The third term represents entropy loss upon magnetization,

$$e(m) = -\ln(1 - m^2) + \frac{m^2}{2} - \frac{m^4}{20} - \frac{53}{1050}m^6 + \dots \quad (2)$$

The final term is the magnetic mean field energy. Note this term couples magnetization to density. We may add on an additional term $-Hm/T$ to represent an applied external field.

The magnetic mean field energy requires further comment. In its derivation we assume magnetization distributed uniformly outside a cavity containing one dipolar sphere, the mean field at the center of the cavity is the integral of the dipole function

$$h(0) = \rho m \int d^3r \frac{3(\hat{m} \cdot \hat{r})^2 - 1}{r^3} \quad (3)$$

over the entire system. Due to the anisotropy of the dipole interaction, this integral vanishes identically over concentric spherical shells centered at the origin. Since the dipole interaction is long ranged, however, the integral depends on the shape of the outer boundary of integration. Taking this shape as a highly prolate spheroid (see Fig. 1) we find that the most remote regions of the system combine to form the nonzero mean field.

We choose this shape for our calculations since it avoids the demagnetizing field of more compact shapes and represents the true thermodynamic limit. The actual shape of a droplet of magnetized fluid represents an important

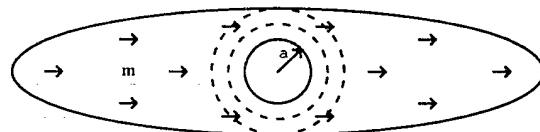


FIG. 1. Geometry for calculating mean field. Outer boundary is a highly prolate spheroid. Inner boundary depends on particle shape. For spherical particles, field at center arises from the most distant regions of the spheroid.

outstanding problem. Presumably surface tension favors a more compact shape. To avoid demagnetizing fields the magnetization may rotate slowly across the sample. Resolution of this open question will assist in finding experiments to reveal a possible magnetized liquid state.

The spherical inner shell reflects the particle shape. For spheroidal particles with axis of rotation a parallel to the dipole moment and axes b perpendicular, the coefficient of ρm^2 in the free energy [Eq. (1)] becomes

$$-\frac{2\pi}{3T} \left(1 - \frac{4}{5}\chi + \dots\right) \quad (4)$$

for small $\chi \equiv (a^2 - b^2)/(a^2 + b^2)$. Thus prolate (needle, $a > b$) shapes inhibit magnetization while oblate (pancake, $b > a$) shapes enhance it.

The coefficient of ρm^2 in the magnetic mean field energy may vary in a structured liquid. The onset of particle chaining, for example, creates a favorable contribution to the magnetic energy from local interactions. Calculating the free energy accurately is an extremely difficult task. We therefore focus, for the remainder of this paper, on generic questions independent of the detailed form of the free energy. We identify three generic phase diagrams for dipolar sphere fluids [see Figs. 2(a)–2(c)]. These differ according to the position T_c^0 of the van der Waals critical point.

When T_c^0 is very high [Fig. 2(a)], we find phase coexistence between a dilute isotropic gas and a dense isotropic liquid, as predicted by the magnetization-independent van der Waals part in our free energy. Several authors [5–7,20–22] studied this phase coexistence caused by the effective $1/r^6$ attraction of the orientationally averaged dipolar interaction. In addition, a continuous magnetic phase transition extends from high temperatures and densities and intersects the phase coexistence boundary. Below this critical end point a dilute isotropic gas and a dense magnetic liquid coexist.

When T_c^0 is very low [Fig. 2(c)], we find a continuous magnetic phase transition at high temperatures and densities crossing over to a first order transition with an associated phase coexistence region. This crossover marks a tricritical point. Phase diagrams of this type arise from mean field theories [15,16] of ferrofluids which neglect attractive forces other than the mean field interaction (i.e., they set $T_c^0 = 0$). Our result shows that even with an isotropic attraction added to mean field attraction, phase coexistence between two isotropic fluids is preempted by the magnetic fluid phase as long as the isotropic attraction is sufficiently weak, in agreement with Sano and Doi [16].

For intermediate values of T_c^0 [Fig. 2(b)], the phase diagram combines the features of the above two phase diagrams giving rise to a triple point at which three phases coexist: a dilute isotropic gas, a dense isotropic liquid, and a dense magnetic liquid. Above the triple point temperature, two isotropic fluids coexist at low and moderate densities, becoming identical above the critical temperature T_c^0 . At higher densities, the isotropic liquid and magnetic liquid are separated by a first order transition which becomes second order above the tricritical temperature. Below the triple point temperature, the isotropic

gas coexists with the magnetic liquid.

An applied field H destroys the continuous magnetic transition. For either high or low values of T_c^0 , the phase diagram consists of a gas-liquid phase coexistence. The field dependent critical point location describes the essentials of the field response of the phase diagram. When T_c^0 is very high [Fig. 2(a)], the critical point originates from the isotropic gas-liquid critical point at zero field. When T_c^0 is very low [Fig. 2(c)], the critical point originates from the tricritical point at zero field. For intermediate values of T_c^0 [Fig. 2(b)], the zero field phase diagram contains both an isotropic gas-liquid critical point and a tricritical point. Therefore the evolution of the phase

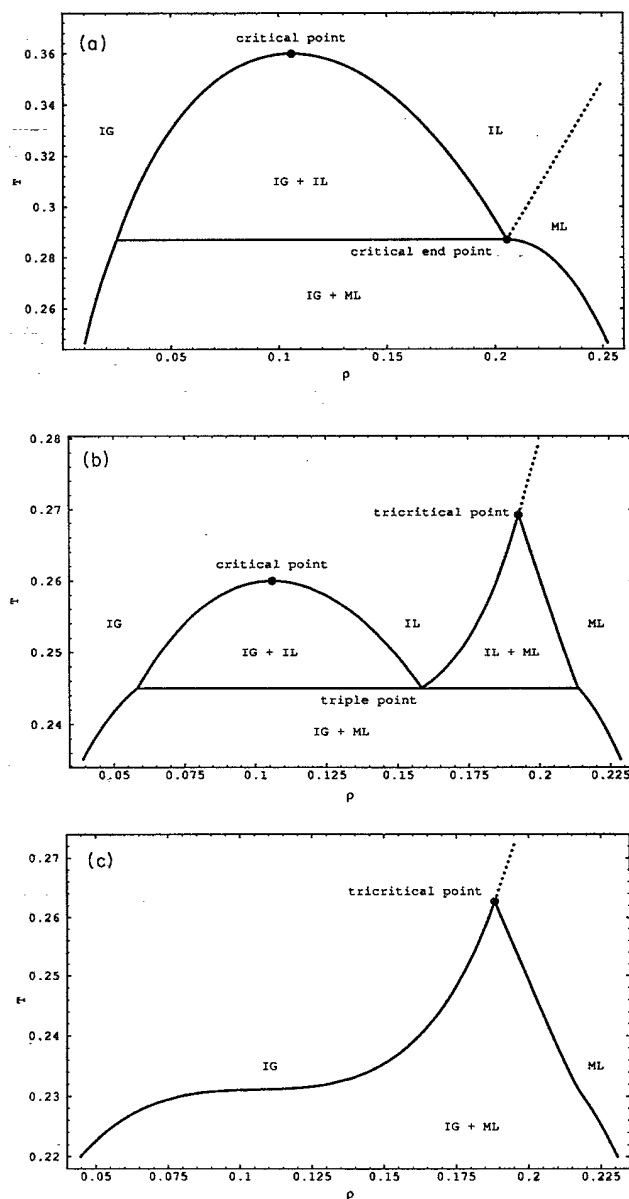


FIG. 2. Generic phase diagrams for dipolar fluids. IG, IL, and ML denote isotropic gas and isotropic and magnetic liquid phases. $\rho_c^0 = 0.106$ in all figures. $T_c^0 = 0.36, 0.26,$ and 0.23 in (a), (b), and (c), respectively. Dotted line denotes continuous transition. Solid lines denote coexistence boundaries. Tie lines are also solid.

diagram for intermediate values of T_c^0 sufficiently illustrates how these two types of critical points change with field strength H .

For intermediate values of T_c^0 [see Figs. 2(b) and 3], the weak field phase diagram contains two critical points, one from the isotropic gas-liquid critical point, and the other from the tricritical point. As we increase the field strength, one of them disappears into the coexistence region of the other, marking a critical end point. We see that the two types of critical points behave differently with applied field. For the critical point stemming from the isotropic gas-liquid critical point, its temperature increases monotonically with field strength H , while its density first increases in a weak field and then turns back to approach the zero field value ρ_c^0 in a stronger field. For the critical point stemming from the tricritical point, its density decreases monotonically with H , while its temperature first lowers in a weak field and then rises in a stronger field.

In summary, we find generic phase diagrams for fluids of dipolar particles. In the absence of intervening liquid-solid transitions one expects continuous magnetization transitions at high temperatures and densities connecting to first order transitions at low temperatures. Phase separation without magnetization is possible but not required. As parameters describing the fluid (such as van der Waals interaction or particle shape) are varied the phase diagrams of Figs. 2(a)–2(c) should occur in sequence. Indeed, analogous sequences are observed in phase diagrams for liquid ^3He - ^4He mixtures [23]. A random field created by immersion in aerogel drives the phase diagrams through this sequence [24]. Another ex-

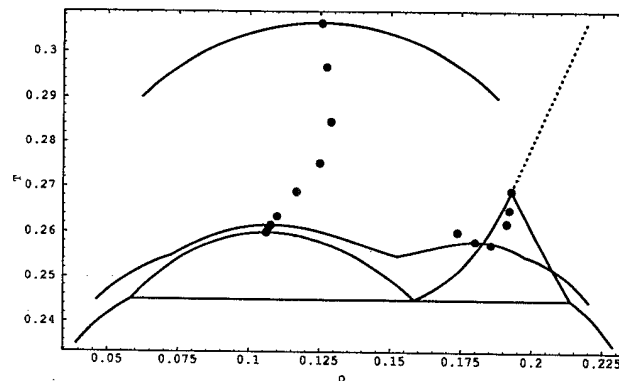


FIG. 3. Evolution of Fig. 2(b) with applied field $H = 0, 0.0002, 0.001, 0.01, 0.02, 0.03, 0.05, 0.07, 0.1, 0.15, 0.2$. Dots locate critical points. Coexistence regions are shown for $H = 0, 0.02, 0.2$ only.

ample is a theory for living polymers in which different solvents correspond to different diagrams in this sequence [25]. If real ferrofluids or other polar fluids actually possess a spontaneously polarized liquid phase, we expect the phase diagram should follow one of the set shown here.

We thank R. B. Griffiths, M. E. Fisher, G. Stell, J. J. Weis, D. Levesque, J. Marko, M. Gingras, M. J. Stevens, and G. S. Grest for useful discussions. This research was supported in part by NSF Grant No. DMR-9221596 and by the A. P. Sloan Foundation.

- [1] J. O. Hirschfelder, C. F. Curtiss, and R. B. Bird, *Molecular Theory of Gases and Liquids* (Wiley, New York, 1954); M. S. Wertheim, *Annu. Rev. Phys. Chem.* **30**, 471 (1979); A. P. Gast and C. F. Zukowsky, *Adv. Colloid Interface Sci.* **30**, 153 (1989); T. C. Halsey and W. Toor, *Phys. Rev. Lett.* **65**, 2820 (1990).
- [2] R. E. Rosensweig, *Ferrohydrodynamics* (Cambridge University Press, Cambridge, England, 1985).
- [3] J. C. Bacri, R. Perzynski, D. Salin, V. Cabuil, and R. Massart, *J. Colloid. Interface Sci.* **132**, 43 (1989).
- [4] P. G. de Gennes and P. A. Pincus, *Phys. Condens. Matter* **11**, 189 (1970).
- [5] G. S. Rushbrooke, G. Stell, and J. S. Hoye, *Mol. Phys.* **26**, 1199 (1973).
- [6] C. E. Woodward and S. Nordholm, *Mol. Phys.* **52**, 973 (1984).
- [7] V. I. Kalikmanov, *Physica A* **183**, 25 (1992).
- [8] M. Widom and H. Zhang, in *Complex Fluids*, edited by E. Sirota, D. Weitz, T. Witten, and J. Israelachvili, MRS Symposia Proceedings No. 248 (Materials Research Society, Pittsburgh, 1992), p. 235.
- [9] P. C. Jordan, *Mol. Phys.* **25**, 961 (1973); D. A. Krueger, *J. Colloid. Interface Sci.* **70**, 558 (1979).
- [10] J. J. Weis and D. Levesque, *Phys. Rev. Lett.* **71**, 2729 (1993).
- [11] M. E. van Leeuwen and B. Smit, *Phys. Rev. Lett.* **71**, 3991 (1993).
- [12] R. E. Rosensweig, *Int. J. Appl. Electromagn. Mater. Suppl.* **2**, 83 (1992).
- [13] G. S. Grest and M. J. Stevens (unpublished).
- [14] H. Zhang and M. Widom, *J. Magn. Magn. Mater.* **122**, 119 (1993).
- [15] A. O. Cebers, *Magnetohydrodynamics* **2**, 42 (1982).
- [16] K. Sano and M. Doi, *J. Phys. Soc. Jpn.* **52**, 2810 (1983).
- [17] M. S. Wertheim, *J. Chem. Phys.* **55**, 4291 (1971).
- [18] J. J. Weis, D. Levesque, and G. J. Zarragoicoechea, *Phys. Rev. Lett.* **69**, 913 (1992).
- [19] D. Wei and G. N. Patey, *Phys. Rev. Lett.* **68**, 2043 (1992).
- [20] P. Frodl and S. Dietrich, *Phys. Rev. A* **45**, 7330 (1992).
- [21] K. C. Ng, J. P. Valleau, G. M. Torrie, and G. N. Patey, *Mol. Phys.* **38**, 781 (1979).
- [22] C. Joslin and S. Goldman, *Mol. Phys.* **79**, 499 (1993).
- [23] M. Blume, V. J. Emery, and R. B. Griffiths, *Phys. Rev. A* **4**, 1071 (1971).
- [24] A. Maritan, M. Cieplak, M. R. Swift, F. Toigo, and J. Banavar, *Phys. Rev. Lett.* **69**, 221 (1992).
- [25] S. J. Kennedy and J. C. Wheeler, *J. Chem. Phys.* **78**, 953 (1983).